



Published in final edited form as:

Prog Mol Biol Transl Sci. 2014 ; 126: 25–51. doi:10.1016/B978-0-12-394624-9.00002-6.

Single-Cell Imaging of Mechanotransduction in Endothelial Cells

Shaoying Lu and Yingxiao Wang

Department of Bioengineering, Institute of Engineering in Medicine, University of California, San Diego, La Jolla, California, USA

Abstract

Endothelial cells (ECs) are constantly exposed to chemical and mechanical microenvironment in vivo. In mechanotransduction, cells can sense and translate the extracellular mechanical cues into intracellular biochemical signals, to regulate cellular processes. This regulation is crucial for many physiological functions, such as cell adhesion, migration, proliferation, and survival, as well as the progression of disease such as atherosclerosis. Here, we overview the current molecular understanding of mechanotransduction in ECs associated with atherosclerosis, especially those in response to physiological shear stress. The enabling technology of live-cell imaging has allowed the study of spatiotemporal molecular events and unprecedented understanding of intracellular signaling responses in mechanotransduction. Hence, we also introduce recent studies on mechanotransduction using single-cell imaging technologies.

1. INTRODUCTION

Mechanical forces play crucial roles in regulating pathophysiological processes, e.g., atherosclerosis, the leading cause of death in the USA and most developed countries.¹ Shear stress without a clear direction can lead to endothelial cell (EC) dysfunction and atherogenesis,^{2–4} but there is a lack of understanding on how ECs perceive the spatiotemporal cues and transduce them into biochemical activities to regulate cellular functions. The underlying pathology of atherosclerosis involves a chronic inflammatory process of vessel wall⁵ due to endothelial dysfunction with increased permeability and recruitment of immune cells, including monocytes, resulting from upregulation of adhesion molecules and cytokine secretion by ECs.⁵ Atherosclerosis occurs preferentially at vascular curvature and branch sites where the vessel walls and ECs are exposed to disturbed flow, which has been reported to facilitate atherogenesis.^{6–8} It is possible that the greater spatiotemporal heterogeneity of shear-stress distribution under atheroprone disturbed flows than that of atheroprotective laminar flows contributes to the pathophysiological modulation of EC responses in the subsequent mechanotransduction.^{2,9–15}

Since the plasma membrane provides an interface between the cell and environment, it is expected to be an important subcellular structure in mechanotransduction. Transmembrane receptors such as integrins, G-protein-coupled receptor (GPCR), platelet endothelial cell adhesion molecule (PECAM-1), and transient receptor potential channels (TRPC6) can be activated by shear to regulate downstream signals, i.e., membrane-associated tyrosine kinases, Ca²⁺, and small GTPases.^{16–18} Shear stress has been shown to activate Src, which leads to ERK activation and translocation between nucleus and cytosol, and subsequent

atheroprone genetic changes.^{19–21} TRPC6 can also sense shear and trigger Ca²⁺ influx to regulate EC permeability.^{22,23} The plasma membrane also consists of different microdomains,²⁴ including lipid rafts,²⁵ which play important roles for mechanotransduction.²⁶ Various mechanosensing elements can localize at or proximal to the plasma membrane to regulate downstream intracellular functions.²⁷

The wide applications of fluorescence proteins (FPs) in single live-cell imaging have revolutionized the whole research field of cell biology, including mechanotransduction in ECs. Fluorescence resonance energy transfer (FRET)-based biosensors have been engineered and applied to molecular activities in live cells.^{28–37} The ratiometric measurement of the biosensors utilizes the ratio of the donor to acceptor fluorescence intensity to represent the target molecular activity. This measurement is self-normalizing and independent of the heterogeneous biosensor expression level among various cells.³⁸ The genetically engineered FRET biosensors also allow subcellular localization to cytosol, plasma membrane, or organelles, which can provide versatile measurement of local molecular activities. As a result, the FRET-based biosensors have been widely used in live cells to monitor molecular signals in real time.^{39,40}

Utilizing fluorescence imaging technologies including FPs and FRET biosensors, a large amount of video imaging data of live cells have been collected. In order to precisely and efficiently interpret the underlying biological mechanism, automated, intelligent, and objective image analysis tools are in high demands.³⁹ Automatic methods for the accurate detection of cell and subcellular features are crucial for the high-throughput image analysis and quantification of subcellular molecular interactions. For example, the water algorithm has been widely used to detect FAs in fluorescent images.^{41–45} Quantitative image-based analysis can also reveal the hidden spatial pattern and temporal sequence of signaling events.^{46,47} Integrated computational tools are needed to quantify the activity and localization of intracellular molecules, which can provide the basis for the quantitative analysis elucidating subcellular molecular interactions and therefore contribution to EC migration and atherosclerosis.^{39,47–49}

2. ATHEROSCLEROSIS, EC WOUND HEALING, AND MECHANOTRANSDUCTION

Atherosclerosis is a cardiovascular disease characterized by the patchy deposit of fatty materials in the arterial walls and reduced/blocked blood flows.⁵⁰ It occurs preferentially at vascular curvature and branch sites where the vessel walls are exposed to disturbed flows, but not at the straight parts of vessels where laminar flows dominate.⁵⁰ Vascular ECs, which form a mono-layer of endothelium lining along and protecting the vessel wall from the circulating blood,⁵¹ are continuously exposed to shear stress resulted from these different flows. It has been shown that ECs subjected to disturbed flows, but not to laminar flows, tend to have a high and sustained permeability, which facilitates the formation of atherosclerosis.^{52,53} Recent evidence also indicates that the effect of disturbed flows on ECs is pro-inflammatory, whereas that of laminar flows is anti-inflammatory.^{50,54–57} For example, disturbed flows induced the expression of pro-inflammatory BMP-4 and cytokines

and adhesion receptors such as intercellular adhesion molecule-1 (ICAM-1) and vascular cell adhesion molecule (VCAM-1).^{58–60} In contrast, laminar flows can inhibit the inflammatory signaling cascades induced by TNF α .^{61–63}

Following the atherosclerosis, the injury of endothelium and loss of ECs after bypass surgery or balloon angioplasty is the main cause of restenosis. The EC wound healing process, which involves EC migration at the wounding edge followed by EC proliferation, serves as the critical step to restore the endothelium integrity and prevent restenosis.⁶⁴ Shear stress has been shown to affect the EC wound healing process by modulating EC junctions. EC junctions in a monolayer can be disrupted by shear stress and recovered if continuously exposed to laminar flows for long term as the cells adapt to the new environment.^{52,53} The transient disruption of cell junctions under laminar flows will last long during the wound healing process because it takes time for cells to repair the wound, restore a stable monolayer, and adapt to the new environment. This junction disruption would hence keep the ECs disengaged from each other and free to move. As such, the laminar flow-directed protrusion and migration of ECs at the upstream side of wounded area can be promoted and maintained before the wound closure, thus facilitating the EC migration toward the wounded area. At the downstream side, the pushing effect of laminar flows on cells along the flow direction negates the junction disruption-induced motility enhancement. Although a wound per se can also induce a migration of cells at both wounding edges to close the wound, results have revealed that laminar flows promote cells at the upstream side to migrate into the wounded area faster, whereas the rate of cell migration downstream of flow is comparable to that without flow.⁶⁵ This asymmetric effect of laminar flows results in an increased net speed of wound healing comparing to that without flow. In fact, both in vitro and in vivo experiments indicate that laminar flows enhance EC migration and consequently wound healing.^{66–68} Laminar flows have been shown to enhance the wound healing by modulating cell–cell and cell–extracellular matrix (ECM) adhesions, in particular, vein endothelial (VE)-cadherin-mediated adherens junction (AJ)^{69,70} and β 1 integrins.⁷¹ Membrane fluidity, cytoskeleton, and tyrosine kinases also appear to be important for the laminar flow-induced EC wound healing.^{65,72,73} Interestingly, disturbed flows induce sustained disruption of AJ.^{52,53} However, the EC migration speed toward the wounded area under disturbed flows is comparable to that without flow.⁶⁵ It was revealed that ECs under disturbed flows have strong staining of focal adhesion proteins due to the unstable mechanical environment,⁶⁵ which may impair the cell detachment from the substrate necessary for EC migration and hence negate the motility enhancement due to the junction disruption.⁷⁴ It remains an intriguing question how ECs coordinate the multiple signaling events in space and time under different flows to regulate AJ, protrusion, motility, migration, and wound healing.

It has been well documented that shear stress can activate a variety of signaling cascades and gene expressions to regulate EC functions and pathophysiological processes.^{7,8,75} For example, a wide range of signaling molecules and structures, including the plasma membrane,^{76,77} membrane proteins/receptors (e.g., integrins,^{16,19} GPCR,¹⁷ cadherin,^{18,53} PECAM-1,^{18,78,79} VCAM-1,^{80,81} ICAM-1,⁸⁰ and ion channels⁷⁵), actin filaments,⁸² microtubules,^{83,84} and intermediate filaments^{85–87} were identified to play important roles in transmitting shear stress into biochemical signaling cascades, i.e., mechanotransduction. Atheroprone disturbed fluid shear stress has been reported to induce the expression of

fibronectin (FN) gene in human ECs and enhance its assembly into fibril matrix.⁸⁸ In particular, the PECAM-1/NF- κ B pathway was found to be essential for FN accumulation in atheroprone regions of the aortic arch, which positively feedbacks and promotes the activation of NF- κ B and atherogenesis.⁸⁸ Evidence also indicates that both the temporal and spatial gradient of shear stress can affect the cellular functions.^{2,10–12,14,15,76,89} In fact, it was realized that the subcellular characteristics of shear stress are heterogeneous in a single cell and impact significantly on cellular responses.^{12,19,90,91} Calcium flux in response to shear stress showed significant subcellular directionality.^{92,93} The lateral diffusion coefficient of lipids in the plasma membrane also increased at regions upstream of the nucleus while decreased at the downstream regions upon shear-stress application.⁹⁴

3. SIGNALING MOLECULES INVOLVED IN MECHANOSENSING AND MECHANOTRANSDUCTION

TRPCs at the plasma membrane can regulate Ca^{2+} entry and play crucial roles in regulating EC actomyosin contractility and permeability^{22,23}; increased TRPC6 expression has been revealed as a hallmark of atherosclerosis⁹⁵ and atheroprone flow shear stress has been shown to induce TRPC6 expression in ECs.⁹⁶ TRPC6 can also interact with caveolin,⁹⁷ which is localized at VE-cadherin-mediated AJs.⁹⁸ In fact, TRPC4, a close family member of TRPC6, has been shown to colocalize with VE-cadherin at AJs.⁹⁹ Therefore, the Ca^{2+} influx mediated by TRPC6 may affect the local $[\text{Ca}^{2+}]$ in the intercellular junction, at least transiently, and modulate VE-cadherin functions to regulate EC permeability. While TRPC6 can mediate the effect of shear stress on triggering the Ca^{2+} influx under different stimuli,¹⁰⁰ it remains controversial whether TRPC6 can be directly activated by mechanical tension¹⁰¹ or indirectly via GPCRs and their effector phospholipase C (PLC).^{102,103} Since shear stress has been reported to stimulate GPCRs and their coupled G-proteins,^{17,104,105} it is possible that shear stress utilizes GPCR/PLC pathway to activate TRPC6 besides imposing direct mechanical impact.

Src kinase is recruited to the plasma membrane and activated differentially at the different membrane microdomains under various conditions (Fig. 2.1).^{34,106} Shear stress can activate Src^{19,107,108} through plasma membrane mechanosomes containing PKG/Shp2.¹⁰⁹ This shear-induced Src can then lead to the phosphorylation and activation of ERK^{21,110,111} via Shc/Grb2/SOS/Ras/MEK pathway.¹⁰⁹ The phosphorylated ERK can translocate into the nucleus¹¹² and undergo an oscillatory translocation between nucleus and cytosol²⁰ to regulate downstream gene expression of MCP-1 for monocyte recruitment.¹¹³ It has been hypothesized that the spatiotemporal patterns of these oscillatory activities of transcription factors can regulate the strength and time course of the target gene expression.²⁰ Recent evidence indicates that molecular functions are dependent on its subcellular localization. For example, Src inhibits Rho GTPase at the focal adhesion sites,¹¹⁴ whereas it activates Rho GTPase at podosomes.¹¹⁵ Furthermore, junction remodeling takes place at a molecularly and phenotypically distinct subset of VE-cadherin adhesions, focal AJs, and vinculin associates with focal AJs and stabilizes the junctions from opening during their force-dependent remodeling.¹¹⁶ Therefore, the different spatiotemporal characteristics of disturbed and laminar flows may cause differential TRPC6 activation and/or Src localization/function at

membrane microdomains to regulate AJs and MCP-1, which modulate endothelial permeability and monocyte recruitment, respectively.⁵

4. THE EFFECT OF SUBCELLULAR STRUCTURE ON MECHANOTRANSDUCTION

The plasma membrane is not uniform in structure²⁴ and has different compartments, e.g., lipid rafts, which are rich in cholesterol, sphingomyelin, and saturated fatty acids.²⁵ These compartment structures and their interaction with cytoskeleton are involved in the regulation of intracellular signaling.²⁶ Indeed, Src family kinase (SFK) members, including Fyn and Lyn, are anchored at lipid rafts to become activated following N-terminal palmitoylation and myristoylation,¹¹⁷ whereas H-Ras depends on the non-rafts anchoring at the plasma membrane to be functional.^{117,118} Evidence also indicates that the plasma membrane and its compartments are involved in mechanotransduction. For example, different subtypes of G-proteins are partitioned into membrane compartments to regulate the mechanical-activated signaling molecules, e.g., nitric oxide production¹¹⁹ and MAPK activity.¹²⁰ The modulation of the plasma membrane fluidity also altered the shear stress-induced MAPK signaling pathway,⁹⁴ further underscoring the importance of the plasma membrane in mechanotransduction.

Src kinase is a nonreceptor tyrosine kinase critical for a variety of cellular processes.¹¹⁴ At resting state, Src localizes at the microtubule-associated perinuclear regions^{34,121–126} and/or at the nonrafts regions on the plasma membrane.^{127–129} Recent evidence indicates that Rho small GTPases and the associated actin network can facilitate the transportation of Src from perinuclear area to actin-associated cell periphery,^{130–132} possibly through the Src SH3 domain, but not the catalytic domain.^{133,134} The inhibition of RhoA or actin stress fibers but not microtubules resulted in the blockage of Src translocation/activation in response to various stimuli.^{130–132} The compartmental structures at the plasma membrane are also involved in the localization and regulation of Src kinase.^{26,135} Indeed, SFKs can be transported to distinct compartments of plasma membrane through different types of endosomes.¹³⁶ SFK members such as Lyn and Fyn can reside in lipid rafts of the plasma membrane,¹³⁷ via their N-terminal myristoylation and palmitoylation sites.¹¹⁸ Src kinase itself has only myristoylation motif and it is not clear whether Src kinase localizes within the lipid rafts at the plasma membrane.^{127–129,138–140} In mouse fibroblasts, Src was shown to be excluded from the detergent-resistant membrane (DRM) fractions in one study, while another publication suggested that Src resides in DRM fraction.^{127,140} Different groups also reported different Src localizations in PC12 cells.^{129,139} This inconsistency is likely attributed to the controversial effects of nonionic detergents and the detergent extraction method used in these reports for isolating DRMs.^{141,142} Advanced methods are hence needed to visualize the Src translocation and activation at different compartments on the plasma membrane in live cells.

Src contributes to cell protrusion and migration in many ways. Src, mediated by focal adhesion kinase (FAK), can phosphorylate p130cas, which recruits Crk and DOCK180 through the interaction of SH3 domain on Crk and PXXP motif on DOCK180. DOCK180

subsequently binds to ELMO and activates Rac, which leads to the activation of Wave1/Scar1.¹⁴³ Recent results indicate that Src can also directly phosphorylate Scar1.¹⁴⁴ Activated Scar1 can bind to and activate Arp2/3, which causes the branching growth of actin filaments and the formation of actin arcs adjacent to the plasma membrane.¹⁴³ The polymerized actin filaments bend beneath membrane, and the subsequently accumulated thermodynamic energy in situ may eventually promote the protrusion of the lipid layer at the leading edge along migration direction.¹⁴⁵ It has been reported that Src can be activated in live human umbilical VE cells by applying laser-tweezer traction on FN-coated beads adhering to the cells.³⁴ A rapid distal Src activation and a slow directional wave propagation of Src activation along the plasma membrane have been observed. The wave propagated away from the stimulation site with a relatively constant speed of about 18.1 nm/s. This force-induced directional and long-range activation of Src can be abolished by the disruption of actin filaments or microtubules. Therefore, the transmission of mechanically induced Src activation is considered a dynamic process that directs signals via the cytoskeleton to spatial destinations (Fig. 2.2).³⁴

The permeability of endothelium and consequently atherosclerosis involves EC junctions.^{69,147} Among the three major types of intercellular connections, viz., AJ, gap junction, and tight junction,¹⁴⁸ AJ is the most ubiquitous.¹⁴⁹ In ECs, AJ is mainly comprised of a membrane receptor VE-cadherin, with its intracellular domain separated into the juxta-membrane domain (JMD) and the catenin-binding domain (CBD). JMD provides putative docking sites for p120^{ctn}, which is a substrate molecule for Src. CBD binds directly to β -catenin and γ -catenin, which possibly bridge the VE-cadherin complex to actin-based cytoskeleton.^{148,150,151}

Active Src perturbs the cadherin-mediated cell–cell adhesion. For example, AJ was severely deteriorated in v-Src transformed fibroblasts.^{152,153} Constitutively active Src protein also caused the tyrosine phosphorylation of E-cadherin and a concurrent loss of cell–cell contact.¹⁵⁴ Further, ERK is constitutively activated in Src-transformed cells.^{110,111} The SH2/SH3 domains of Src can recruit¹⁵⁵ and activate ERK, resulting in the phosphorylation of an ERK substrate molecule myosin light-chain kinase (MLCK).¹¹⁷ The phosphorylation of MLCK ultimately leads to the phosphorylation of myosin light chain and activation of actomyosin machinery to cause the in situ contractility and the breakage of AJ.¹⁵⁵ Shear stress has been shown to activate both Src and ERK in bovine aortic endothelial cells (BAECs).^{19,107,156} It is, however, not clear how different flows activate Src, ERK, and MLCK in space and time to regulate AJ.

5. FOCAL ADHESION AND FAK

Focal adhesions are the contact sites of cells to outside ECM through transmembrane proteins integrins. Integrins are heterodimeric receptors containing α and β subunits, and so far 24 different subtypes of integrins have been identified in vertebrates with the combination of 18 α and 8 β subunits. These integrin subtypes allow the diverse and specific recognition of various ECM proteins, e.g., FN, fibrinogen, collagen, vitronectin, and laminin.¹⁵⁷

After the ligation of integrins with ECM proteins, many structural and signaling proteins are recruited to focal adhesions. Signaling proteins at focal adhesions include kinases, e.g., Src, FAK, integrin-linked kinase, and phosphatase, e.g., receptor-like tyrosine phosphatase α . Since integrin itself lacks the enzymatic activity, these signaling proteins at focal adhesions are crucial to transfer extracellular mechanical information inside the cells. For example, integrin-mediated activation of Src and FAK can regulate Rho GTPases, which then regulate the organization of actin cytoskeleton.^{158,159} Src and FAK coordinate and regulate downstream signals in focal adhesions (Fig. 2.2).^{146,160} It has been reported that growth factor-induced FAK activation is mediated and maintained by Src activity, while FAK activation on cell adhesion is independent of and in fact essential for the Src activation.¹⁴⁶ FAK also interacts with integrin receptors and ECM proteins to sense the mechano-environment (Fig. 2.2).¹⁶⁰ Seong et al. found that matrix protein FN-mediated FAK activation is dependent on mechanical tension, which may expose the otherwise hidden FN synergy site to integrin α 5. In contrast, the binding motif of type I collagen to its receptor integrin α 2 is constitutively exposed. Hence, FAK can be sufficiently activated on type I collagen independent of tension. Therefore, different ECM proteins can differentially transmit or shield mechanical forces from the environment to the functional molecules in the cell and regulate cellular functions (Fig. 2.2).¹⁶⁰

Structural proteins, for example, talin, paxillin, vinculin, and zyxin, link other focal adhesion proteins and actin cytoskeleton. For example, ECM-bound integrins can recruit an adaptor molecule talin to focal adhesions. Talin has the binding sites for another molecule vinculin, which then bind to actin cytoskeleton.^{161,162} As such, outside ECM can be physically connected to intracellular cytoskeleton through integrin and focal adhesion proteins. Therefore, due to their physical location at the interface between extracellular microenvironments and intracellular space, focal adhesions play crucial roles in sensing mechanical signals from both outside and inside.^{163,164}

6. TOOLS TO MONITOR SIGNAL TRANSDUCTION IN LIVE CELLS

6.1. FPs, FRET, and fluorescence lifetime imaging microscopy

Molecular-tagged FPs and specific FRET biosensors are capable of monitoring cellular events in live cells.^{28–37} YPet, a variant of yellow FP, was paired with enhanced cyan fluorescence protein (ECFP) and severalfolds increase in sensitivity was observed for various biosensors.^{165,166} These ECFP/YPet-based biosensors, however, only allow the visualization of one active molecular event in a single live cell. Several studies have used one FP as the common donor or acceptor for two FRET biosensors to visualize different molecular signals in the same cell.^{167–169} Other pairs, including Ametrine paired with tdTomato,¹⁷⁰ mOrange with mCherry,^{171–174} TagFP with mPlum,¹⁷⁵ and T-Sapphire with DsRed,¹⁷⁶ have been explored as a second FRET pair.^{171–174} These approaches either require sophisticated means to quantify the signals or are difficult for multi-FRET imaging in a single cell. The potential of mOrange2/mCherry as a new FRET pair, together with ECFP and YPet, was also demonstrated for dual-FRET imaging.¹⁷⁷

Although mOrange2 and mCherry can act as a new FRET pair to monitor active signaling events,¹⁶⁶ there is some overlap between their excitation spectra to cause nonspecific cross

talk,^{171,172} and this may have contributed to the lower sensitivity of a MT1-MMP FRET biosensor in vitro using the mOrange2/mCherry pair.¹⁶⁶ Because fluorescence lifetime imaging microscopy (FLIM) only monitors the donor lifetime to measure FRET signals without the need to measure the acceptor lifetime, it can avoid the nonspecific contamination of acceptor excitation/emission. FLIM is also independent of the local concentrations of fluorescent molecules and can separate the population of “FRETing” donors from those of noninteracting ones based on the lifetime distribution, thus enhancing the accuracy of FRET detection.^{178–181} Hence, FLIM is ideal for the visualization of multiple FRET biosensors simultaneously in the same live cell.

Recently, FRET techniques have been applied to visualize signal transduction in response to shear stress. For example, GFP-fused Rac and Alexa568-p21-binding domain of PAK1 (PBD) were used to monitor the Rac activation in live cell by measuring FRET between GFP to Alexa568.¹⁸² With this FRET-based biosensor, shear stress was shown to induce a directional activation of Rac concentrated at the leading edge of the cell along flow direction.¹⁸³ Shear stress has also been shown to induce a polarized Cdc42 activation along flow direction visualized by the FRET between a GFP-Cdc42 and an Alexa568-PBD.¹⁸⁴ In another study, a separated pair of ECFP-fused relA and EYFP-fused I κ B α was used to monitor the interaction of relA and I κ B α . The FRET efficiency between ECFP-relA and EYFP-I κ B α decreased upon shear-stress application, indicating a mechanical force-induced dissociation of relA and I κ B α .¹⁸⁵ CFP and YFP have also been fused to human B₂ bradykinin receptor, a GPCR, to detect the activation of GPCR. Shear stress was shown to activate B₂ bradykinin GPCR within 2 min, which can be inhibited by B₂-selective antagonist.¹⁷ These results suggest that B₂ bradykinin GPCR may serve as a mechanosensing molecule in response to shear stress. In the mechanosensing and mechanotransducing elements included focal adhesion and the cytoskeleton network, FRET biosensors have been developed for many molecules, including Src, FAK, α -actinin, vinculin, and talin.^{34,146,186}

6.2. Quantitative image-based analysis for live cells

The development and application of FPs and related biosensors have greatly advanced our knowledge of signaling transduction in live cells. The vast amount of imaging data produced by these FPs and biosensors demands the development of automated, intelligent, and objective image analysis tools to allow precise and efficient interpretation of complex biological information.^{39,44} Automated algorithms integrated with image-based analysis have been developed and utilized to analyze the kinetics of FPs, discretize the intracellular space, track the cell movement, and detect the localization of the FPs. Here, we briefly review the widely used fluorescence recovery after photobleach (FRAP) analysis methods for quantifying the diffusion kinetics of molecules and provide an example of quantitative polarity analysis based on images.

6.3. The FRAP analysis and finite-element-based diffusion analysis

The diffusion kinetics of a FRET biosensor, or a fluorescent molecule, can be examined by FRAP analysis, a widely used technique in estimating the apparent diffusion coefficient of molecules in live cells.^{187–190} In classical FRAP analysis, the fluorescence recovery curve is

obtained by monitoring the recovery process of the average fluorescence intensity in the small region, which underwent photobleaching and the subsequent recovery. The apparent diffusion coefficient of fluorescent molecules can be estimated by performing parameter fitting on the recovery curve.¹⁸⁷ Results from the FRAP analysis has been revealed the characteristics of transport kinetics for many important molecules.^{190–192} However, there are limitations with this approach on the geometry of the cell, the geometry of the photobleached spot, and the actual photobleaching process that can be analyzed.^{187–189,193} Most recently, FRAP analysis using computational approaches, such as the model-based finite-element (FE) and finite-difference methods and the simulation-based computational particle and Monte Carlo methods, has been developed to address these limitations.^{192,194–200}

In particular, the FE method is a computational approach for defining a set of linear equations, which approximate the partial differential equations in the value of solutions. It is well known for the flexibility in resolving complex geometry of tissue and cellular structures for approximating the elastic and diffusion equations.^{201,202} This method has been used to estimate the apparent diffusion constant in inhomogeneous tissues²⁰⁰ and model protein transport in single cells.²⁰³ Newly developed FE-based image analysis and simulation tool for FRAP enforce no specific requirement on the geometry of cell, the bleaching light beam, or the photo-bleaching process. This tool provided a general approach for evaluating the accuracy of the diffusion model. With this FE-based tool integrated with diffusion model, the diffusion of FRET-based Src biosensors has been evaluated, simulated, and subsequently subtracted from the biosensor FRET signals in live cells.⁴⁶

6.4. Automatic tracking of moving cells and subcellular features

Image registration is the process of transforming different sets of images into one coordinate system. It is widely used in engineering and science for automatically finding the pixel-wise transformation from the data to reference images by detecting and matching their feature points and the interpolation of values among these feature points.^{204,205} For example, it was used in live-cell FRET imaging to physically align the fluorescent images obtained at different wavelengths simultaneously.^{31,182,206} However, the registration of the video images of moving cells is a considerably more challenging problem, due to the relatively nonlinear movement of cell body during migration or adhesion. To circumvent the difficulty involved in the image registration of moving cells, some quantification methods have been developed to divide the whole cell into small wedges in the polar coordinated system and quantify the cell motility, protein distribution, or molecular activity in these wedges with different fixed angles.^{206–208} These methods are very useful to align and quantify the molecular localization in the angular direction among different cells or in a cell which changes the shape in time. However, a robust and accurate whole-cell image registration method capable of tracking all intracellular pixels is needed for the precise image analysis and model simulation of molecular activities in migrating cells.

In addition to whole-cell analysis, it is very important to detect and track molecular locations and activities within subcellular structures. For example, the image segmentation-based water algorithm has been developed to detect individual FAs based on their intensity

profiles. It was initially used to characterize the molecular heterogeneity between and within FAs and to study the effect of kinase inhibitors on FA disassembly.⁴¹ It was also applied successfully for analyzing the correlation between the local force and the physical property of FAs in subcellular locations, such as orientation, size, and shape.⁴² This algorithm has further helped to discover that the FA dynamics is regulated by the pattern of integrin clusters,²⁰⁹ and to characterize the effect of different drugs on the structure and organization of FAs in a high-throughput fashion.⁴³

Polarized molecular activities play important roles in guiding the cell toward persistent and directional migration as those observed in wound healing and the growth of blood vessels. Molecular polarity has been quantified using automated analysis method, and the related time difference among different molecules can be used to compare the time sequence in the signaling pathways (Fig. 2.3).^{46,47} Lu et al. showed the polarized distributions of the activities of phosphatidylinositol 3-kinase (PI3K) and the Rac1 small GTPase monitored using chimeric FPs in cells. The cells were constrained on micropatterned strips, with one end connecting to a neighboring cell (junction end) and the other end free of cell–cell contact (free end, see Fig. 2.3). The subcellular distribution of FPs and the edge position and velocity at the free end of the cells were quantified to analyze their correlation and interpret the signaling sequence. The initiation of the edge extension occurred before the activation of PI3K, which led to a stable extension of the free end followed by the Rac1 activation.⁴⁷ The results showed the power of quantitative image-based analysis in deciphering coordinated sequential signaling events regulating the lamellipodia extension and migration in live cells.⁴⁷

7. CONCLUSION

ECs can sense the mechanical force from the environment and convert it into molecular signals regulating cellular function. Studies on the regulation and function, especially mechanotransduction, of ECs provide important insights into the prevention and treatment of cardiovascular diseases such as atherosclerosis. Many molecules function at the plasma membrane or focal adhesions at the interface between the cell and the environment, acting as mechanosensors. Transmembrane receptors and focal adhesion-associated molecules, such as integrin, CGPR, PECAM-1, TRPC6, Src, FAK, p130Cas, and vinculin, are examples of mechanotransducing molecules sensitive to shear stress, stretch, or the stiffness of the microenvironment. Novel technologies such as fluorescence imaging and FRET biosensors provide powerful tools to study the cellular and molecular functions with high spatiotemporal resolution at the single-cell level. Quantitative image-based analysis tools allow the systematic quantification and inference of single-cell imaging results with rigor and accuracy. Therefore, the future in single-cell imaging of mechanotransduction will be illuminated by genetic engineered fluorescence biosensors, which enables the systematic and quantitative exploration of molecular networks in live cells.

References

1. Makowski L, Hotamisligil GS. Fatty acid binding proteins—the evolutionary crossroads of inflammatory and metabolic responses. *J Nutr Sep.* 2004; 134(9):2464S–2468S.

2. Bao X, Clark CB, Frangos JA. Temporal gradient in shear-induced signaling pathway: involvement of MAP kinase, c-fos, and connexin43. *Am J Physiol Heart Circ Physiol*. 2000; 278(5):H1598–H1605. [PubMed: 10775139]
3. Bao X, Lu C, Frangos JA. Temporal gradient in shear but not steady shear stress induces PDGF-A and MCP-1 expression in endothelial cells: role of NO, NF kappa B, and egr-1. *Arterioscler Thromb Vasc Biol*. 1999; 19(4):996–1003. [PubMed: 10195928]
4. Gimbrone MA Jr, Garcia-Cardena G. Vascular endothelium, hemodynamics, and the pathobiology of atherosclerosis. *Cardiovasc Pathol*. 2013; 22(1):9–15. [PubMed: 22818581]
5. Weber C, Noels H. Atherosclerosis: current pathogenesis and therapeutic options. *Nat Med*. 2011; 17(11):1410–1422. [PubMed: 22064431]
6. Tartaglia M, Gelb BD. Noonan syndrome and related disorders: genetics and pathogenesis. *Annu Rev Genomics Hum Genet*. 2005; 6:45–68. [PubMed: 16124853]
7. Davies PF, Spaan JA, Krams R. Shear stress biology of the endothelium. *Ann Biomed Eng*. 2005; 33(12):1714–1718. [PubMed: 16389518]
8. Boo YC, Jo H. Flow-dependent regulation of endothelial nitric oxide synthase: role of protein kinases. *Am J Physiol Cell Physiol*. 2003; 285(3):C499–C508. [PubMed: 12900384]
9. Li S, Butler P, Wang Y, et al. The role of the dynamics of focal adhesion kinase in the mechanotaxis of endothelial cells. *Proc Natl Acad Sci USA*. 2002; 99(6):3546–3551. [PubMed: 11891289]
10. Butler PJ, Weinbaum S, Chien S, Lemons DE. Endothelium-dependent, shear-induced vasodilation is rate-sensitive. *Microcirculation*. 2000; 7(1):53–65. [PubMed: 10708337]
11. Davies PF. Overview: temporal and spatial relationships in shear stress-mediated endothelial signalling. *J Vasc Res*. 1997; 34(3):208–211. [PubMed: 9226302]
12. DePaola N, Gimbrone MA Jr, Davies PF, Dewey CF Jr. Vascular endothelium responds to fluid shear stress gradients. *Arterioscler Thromb*. 1992; 12(11):1254–1257. [PubMed: 1420084]
13. Frangos JA, Huang TY, Clark CB. Steady shear and step changes in shear stimulate endothelium via independent mechanisms—superposition of transient and sustained nitric oxide production. *Biochem Biophys Res Commun*. 1996; 224(3):660–665. [PubMed: 8713104]
14. Nagel T, Resnick N, Dewey CF Jr, Gimbrone MA Jr. Vascular endothelial cells respond to spatial gradients in fluid shear stress by enhanced activation of transcription factors. *Arterioscler Thromb Vasc Biol*. 1999; 19(8):1825–1834. [PubMed: 10446060]
15. Tardy Y, Resnick N, Nagel T, Gimbrone MA Jr, Dewey CF Jr. Shear stress gradients remodel endothelial monolayers in vitro via a cell proliferation-migration-loss cycle. *Arterioscler Thromb Vasc Biol*. 1997; 17(11):3102–3106. [PubMed: 9409299]
16. Tzima E, del Pozo MA, Shattil SJ, Chien S, Schwartz MA. Activation of integrins in endothelial cells by fluid shear stress mediates Rho-dependent cytoskeletal alignment. *EMBO J*. 2001; 20(17):4639–4647. [PubMed: 11532928]
17. Chachisvilis M, Zhang YL, Frangos JA. G protein-coupled receptors sense fluid shear stress in endothelial cells. *Proc Natl Acad Sci USA*. 2006; 103(42):15463–15468. [PubMed: 17030791]
18. Tzima E, Irani-Tehrani M, Kiosses WB, et al. A mechanosensory complex that mediates the endothelial cell response to fluid shear stress. *Nature*. 2005; 437(7057):426–431. [PubMed: 16163360]
19. Jalali S, Li YS, Sotoudeh M, et al. Shear stress activates p60src-Ras-MAPK signaling pathways in vascular endothelial cells. *Arterioscler Thromb Vasc Biol*. 1998; 18(2):227–234. [PubMed: 9484987]
20. Shankaran H, Ippolito DL, Chrisler WB, et al. Rapid and sustained nuclear-cytoplasmic ERK oscillations induced by epidermal growth factor. *Mol Syst Biol*. 2009; 5:332. [PubMed: 19953086]
21. Brunton VG, Avizienyte E, Fincham VJ, et al. Identification of Src-specific phosphorylation site on focal adhesion kinase: dissection of the role of Src SH2 and catalytic functions and their consequences for tumor cell behavior. *Cancer Res*. 2005; 65(4):1335–1342. [PubMed: 15735019]
22. Singh I, Knezevic N, Ahmmed GU, Kini V, Malik AB, Mehta D. Galphaq-TRPC6-mediated Ca²⁺ entry induces RhoA activation and resultant endothelial cell shape change in response to thrombin. *J Biol Chem*. 2007; 282(11):7833–7843. [PubMed: 17197445]
23. Tiruppathi C, Ahmmed GU, Vogel SM, Malik AB. Ca²⁺ signaling, TRP channels, and endothelial permeability. *Microcirculation*. 2006; 13(8):693–708. [PubMed: 17085428]

24. Simons K, Vaz WL. Model systems, lipid rafts, and cell membranes. *Annu Rev Biophys Biomol Struct.* 2004; 33:269–295. [PubMed: 15139814]
25. Bickett DM, Green MD, Berman J, et al. A high throughput fluorogenic substrate for interstitial collagenase (MMP-1) and gelatinase (MMP-9). *Anal Biochem.* 1993; 212(1):58–64. [PubMed: 8368516]
26. Jacobson K, Mouritsen OG, Anderson RG. Lipid rafts: at a crossroad between cell biology and physics. *Nat Cell Biol.* 2007; 9(1):7–14. [PubMed: 17199125]
27. Chiu JJ, Chien S. Effects of disturbed flow on vascular endothelium: pathophysiological basis and clinical perspectives. *Physiol Rev.* 2011; 91(1):327–387. [PubMed: 21248169]
28. Kunkel MT, Ni Q, Tsien RY, Zhang J, Newton AC. Spatiotemporal dynamics of protein kinase B/Akt signaling revealed by a genetically encoded fluorescent reporter. *J Biol Chem.* 2005; 280(7):5581–5587. [PubMed: 15583002]
29. Miyawaki A, Llopis J, Heim R, et al. Fluorescent indicators for Ca^{2+} based on green fluorescent proteins and calmodulin. *Nature.* 1997; 388(6645):882–887. [PubMed: 9278050]
30. Mochizuki N, Yamashita S, Kurokawa K, et al. Spatio-temporal images of growth-factor-induced activation of Ras and Rap1. *Nature.* 2001; 411(6841):1065–1068. [PubMed: 11429608]
31. Pertz O, Hodgson L, Klemke RL, Hahn KM. Spatiotemporal dynamics of RhoA activity in migrating cells. *Nature.* 2006; 440(7087):1069–1072. [PubMed: 16547516]
32. Ting AY, Kain KH, Klemke RL, Tsien RY. Genetically encoded fluorescent reporters of protein tyrosine kinase activities in living cells. *Proc Natl Acad Sci USA.* 2001; 98(26):15003–15008. [PubMed: 11752449]
33. Violin JD, Zhang J, Tsien RY, Newton AC. A genetically encoded fluorescent reporter reveals oscillatory phosphorylation by protein kinase C. *J Cell Biol.* 2003; 161(5):899–909. [PubMed: 12782683]
34. Wang Y, Botvinick EL, Zhao Y, et al. Visualizing the mechanical activation of Src. *Nature.* 2005; 434(7036):1040–1045. [PubMed: 15846350]
35. Zhang J, Hupfeld CJ, Taylor SS, Olefsky JM, Tsien RY. Insulin disrupts beta-adrenergic signalling to protein kinase A in adipocytes. *Nature.* 2005; 437(7058):569–573. [PubMed: 16177793]
36. Zhang J, Ma Y, Taylor SS, Tsien RY. Genetically encoded reporters of protein kinase A activity reveal impact of substrate tethering. *Proc Natl Acad Sci USA.* 2001; 98(26):14997–15002. [PubMed: 11752448]
37. Buranachai C, Kamiyama D, Chiba A, Williams BD, Clegg RM. Rapid frequency-domain FLIM spinning disk confocal microscope: lifetime resolution, image improvement and wavelet analysis. *J Fluoresc.* 2008; 18(5):929–942. [PubMed: 18324453]
38. Liao X, Lu S, Zhuo Y, Winter C, Xu W, Wang Y. Visualization of Src and FAK activity during the differentiation process from HMSCs to osteoblasts. *PLoS One.* 2012; 7(8):e42709.
39. Wang Y, Shyy JY, Chien S. Fluorescence proteins, live-cell imaging, and mechanobiology: seeing is believing. *Annu Rev Biomed Eng.* 2008; 10:1–38. [PubMed: 18647110]
40. Song Y, Madahar V, Liao J. Development of FRET assay into quantitative and high-throughput screening technology platforms for protein-protein interactions. *Ann Biomed Eng.* 2011; 39(4):1224–1234. [PubMed: 21174150]
41. Zamir E, Katz BZ, Aota S, Yamada KM, Geiger B, Kam Z. Molecular diversity of cell-matrix adhesions. *J Cell Sci.* 1999; 112(Pt 11):1655–1669. [PubMed: 10318759]
42. Balaban NQ, Schwarz US, Riveline D, et al. Force and focal adhesion assembly: a close relationship studied using elastic micropatterned substrates. *Nat Cell Biol.* 2001; 3(5):466–472. [PubMed: 11331874]
43. Paran Y, Ilan M, Kashman Y, et al. High-throughput screening of cellular features using high-resolution light-microscopy; application for profiling drug effects on cell adhesion. *J Struct Biol.* 2007; 158(2):233–243. [PubMed: 17321150]
44. Peng H. Bioimage informatics: a new area of engineering biology. *Bioinformatics.* 2008; 24(17):1827–1836. [PubMed: 18603566]
45. Jaqaman K, Loerke D, Mettlen M, et al. Robust single-particle tracking in live-cell time-lapse sequences. *Nat Methods.* 2008; 5(8):695–702. [PubMed: 18641657]

46. Lu S, Ouyang M, Seong J, Zhang J, Chien S, Wang Y. The spatiotemporal pattern of Src activation at lipid rafts revealed by diffusion-corrected FRET imaging. *PLoS Comput Biol*. 2008; 4(7):e1000127. [PubMed: 18711637]
47. Lu S, Wang Y, Huang H, et al. Quantitative FRET imaging to visualize the invasiveness of live breast cancer cells. *PLoS One*. 2013; 8(3):e58569. [PubMed: 23516511]
48. Sabouri-Ghomi M, Wu Y, Hahn K, Danuser G. Visualizing and quantifying adhesive signals. *Curr Opin Cell Biol*. 2008; 20(5):541–550. [PubMed: 18586481]
49. Machacek M, Hodgson L, Welch C, et al. Coordination of Rho GTPase activities during cell protrusion. *Nature*. 2009; 461(7260):99–103. [PubMed: 19693013]
50. Chien S. Effects of disturbed flow on endothelial cells. *Ann Biomed Eng*. 2008; 36(4):554–562. [PubMed: 18172767]
51. Chien S, Li S, Shyy YJ. Effects of mechanical forces on signal transduction and gene expression in endothelial cells. *Hypertension*. 1998; 31(1 Pt 2):162–169. [PubMed: 9453297]
52. Noria S, Cowan DB, Gotlieb AI, Langille BL. Transient and steady-state effects of shear stress on endothelial cell adherens junctions. *Circ Res*. 1999; 85(6):504–514. [PubMed: 10488053]
53. Miao H, Hu YL, Shiu YT, et al. Effects of flow patterns on the localization and expression of VE-cadherin at vascular endothelial cell junctions: in vivo and in vitro investigations. *J Vasc Res*. 2005; 42(1):77–89. [PubMed: 15637443]
54. Hahn C, Schwartz MA. The role of cellular adaptation to mechanical forces in atherosclerosis. *Arterioscler Thromb Vasc Biol*. 2008; 28(12):2101–2107. [PubMed: 18787190]
55. Berk BC, Abe JI, Min W, Surapisitchat J, Yan C. Endothelial atheroprotective and anti-inflammatory mechanisms. *Ann N Y Acad Sci*. 2001; 947:93–109. discussion 109–111. [PubMed: 11795313]
56. Jo H, Song H, Mowbray A. Role of NADPH oxidases in disturbed flow- and BMP4-induced inflammation and atherosclerosis. *Antioxid Redox Signal*. 2006; 8(9–10):1609–1619. [PubMed: 16987015]
57. World CJ, Garin G, Berk B. Vascular shear stress and activation of inflammatory genes. *Curr Atheroscler Rep*. 2006; 8(3):240–244. [PubMed: 16640961]
58. Chang K, Weiss D, Suo J, et al. Bone morphogenic protein antagonists are coexpressed with bone morphogenic protein 4 in endothelial cells exposed to unstable flow in vitro in mouse aortas and in human coronary arteries: role of bone morphogenic protein antagonists in inflammation and atherosclerosis. *Circulation*. 2007; 116(11):1258–1266. [PubMed: 17785623]
59. Sorescu GP, Song H, Tressel SL, et al. Bone morphogenic protein 4 produced in endothelial cells by oscillatory shear stress induces monocyte adhesion by stimulating reactive oxygen species production from a nox1-based NADPH oxidase. *Circ Res*. 2004; 95(8):773–779. [PubMed: 15388638]
60. Brooks AR, Lelkes PI, Rubanyi GM. Gene expression profiling of vascular endothelial cells exposed to fluid mechanical forces: relevance for focal susceptibility to atherosclerosis. *Endothelium*. 2004; 11(1):45–57. [PubMed: 15203878]
61. Ouyang M, Lu S, Li XY, et al. Visualization of polarized membrane type 1 matrix metalloproteinase activity in live cells by fluorescence resonance energy transfer imaging. *J Biol Chem*. 2008; 283(25):17740–17748. [PubMed: 18441011]
62. Yamawaki H, Lehoux S, Berk BC. Chronic physiological shear stress inhibits tumor necrosis factor-induced proinflammatory responses in rabbit aorta perfused ex vivo. *Circulation*. 2003; 108(13):1619–1625. [PubMed: 12963644]
63. Yamawaki H, Pan S, Lee RT, Berk BC. Fluid shear stress inhibits vascular inflammation by decreasing thioredoxin-interacting protein in endothelial cells. *J Clin Invest*. 2005; 115(3):733–738. [PubMed: 15696199]
64. Schwartz SM, Gajdusek CM, Reidy MA, Selden SC 3rd, Haudenschild CC. Maintenance of integrity in aortic endothelium. *Fed Proc*. 1980; 39(9):2618–2625. [PubMed: 7398892]
65. Hsu PP, Li S, Li YS, et al. Effects of flow patterns on endothelial cell migration into a zone of mechanical denudation. *Biochem Biophys Res Commun*. 2001; 285(3):751–759. [PubMed: 11453657]

66. Albuquerque ML, Waters CM, Savla U, Schnaper HW, Flozak AS. Shear stress enhances human endothelial cell wound closure in vitro. *Am J Physiol Heart Circ Physiol.* 2000; 279(1):H293–H302. [PubMed: 10899069]
67. Sprague EA, Luo J, Palmaz JC. Human aortic endothelial cell migration onto stent surfaces under static and flow conditions. *J Vasc Interv Radiol.* 1997; 8(1 Pt 1):83–92. [PubMed: 9025045]
68. Wu MH, Kouchi Y, Onuki Y, et al. Effect of differential shear stress on platelet aggregation, surface thrombosis, and endothelialization of bilateral carotid-femoral grafts in the dog. *J Vasc Surg.* 1995; 22(4):382–390. discussion 390–382. [PubMed: 7563399]
69. Albuquerque ML, Flozak AS. Wound closure in sheared endothelial cells is enhanced by modulation of vascular endothelial-cadherin expression and localization. *Exp Biol Med (Maywood).* 2002; 227(11):1006–1016. [PubMed: 12486211]
70. Kondapalli J, Flozak AS, Albuquerque ML. Laminar shear stress differentially modulates gene expression of p120 catenin, Kaiso transcription factor, and vascular endothelial cadherin in human coronary artery endothelial cells. *J Biol Chem.* 2004; 279(12):11417–11424. [PubMed: 14699141]
71. Albuquerque ML, Flozak AS. Lamellipodial motility in wounded endothelial cells exposed to physiologic flow is associated with different patterns of beta1-integrin and vinculin localization. *J Cell Physiol.* 2003; 195(1):50–60. [PubMed: 12599208]
72. Albuquerque ML, Flozak AS. Patterns of living beta-actin movement in wounded human coronary artery endothelial cells exposed to shear stress. *Exp Cell Res.* 2001; 270(2):223–234. [PubMed: 11640886]
73. Gojova A, Barakat AI. Vascular endothelial wound closure under shear stress: role of membrane fluidity and flow-sensitive ion channels. *J Appl Physiol.* 2005; 98(6):2355–2362. [PubMed: 15705727]
74. Lauffenburger DA, Horwitz AF. Cell migration: a physically integrated molecular process. *Cell.* 1996; 84(3):359–369. [PubMed: 8608589]
75. Li YS, Haga JH, Chien S. Molecular basis of the effects of shear stress on vascular endothelial cells. *J Biomech.* 2005; 38(10):1949–1971. [PubMed: 16084198]
76. Butler PJ, Norwich G, Weinbaum S, Chien S. Shear stress induces a time- and position-dependent increase in endothelial cell membrane fluidity. *Am J Physiol Cell Physiol.* 2001; 280(4):C962–C969. [PubMed: 11245613]
77. McCabe JB, Berthiaume LG. Functional roles for fatty acylated amino-terminal domains in subcellular localization. *Mol Biol Cell.* 1999; 10(11):3771–3786. [PubMed: 10564270]
78. Bagi Z, Frangos JA, Yeh JC, White CR, Kaley G, Koller A. PECAM-1 mediates NO-dependent dilation of arterioles to high temporal gradients of shear stress. *Arterioscler Thromb Vasc Biol.* 2005; 25(8):1590–1595. [PubMed: 15890968]
79. Fleming I, Fisslthaler B, Dixit M, Busse R. Role of PECAM-1 in the shear-stress-induced activation of Akt and the endothelial nitric oxide synthase (eNOS) in endothelial cells. *J Cell Sci.* 2005; 118(Pt 18):4103–4111. [PubMed: 16118242]
80. Chen CN, Chang SF, Lee PL, et al. Neutrophils, lymphocytes, and monocytes exhibit diverse behaviors in transendothelial and subendothelial migrations under coculture with smooth muscle cells in disturbed flow. *Blood.* 2006; 107(5):1933–1942. [PubMed: 16293605]
81. Nagel T, Resnick N, Atkinson WJ, Dewey CF Jr, Gimbrone MA Jr. Shear stress selectively upregulates intercellular adhesion molecule-1 expression in cultured human vascular endothelial cells. *J Clin Invest.* 1994; 94(2):885–891. [PubMed: 7518844]
82. Li S, Kim M, Hu YL, et al. Fluid shear stress activation of focal adhesion kinase. Linking to mitogen-activated protein kinases. *J Biol Chem.* 1997; 272(48):30455–30462. [PubMed: 9374537]
83. Malek AM, Izumo S. Mechanism of endothelial cell shape change and cytoskeletal remodeling in response to fluid shear stress. *J Cell Sci.* 1996; 109(Pt 4):713–726. [PubMed: 8718663]
84. Morita T, Kurihara H, Maemura K, Yoshizumi M, Yazaki Y. Disruption of cytoskeletal structures mediates shear stress-induced endothelin-1 gene expression in cultured porcine aortic endothelial cells. *J Clin Invest.* 1993; 92(4):1706–1712. [PubMed: 8408624]
85. Helmke BP, Davies PF. The cytoskeleton under external fluid mechanical forces: hemodynamic forces acting on the endothelium. *Ann Biomed Eng.* 2002; 30(3):284–296. [PubMed: 12051614]

86. Helmke BP, Thakker DB, Goldman RD, Davies PF. Spatiotemporal analysis of flow-induced intermediate filament displacement in living endothelial cells. *Biophys J.* 2001; 80(1):184–194. [PubMed: 11159394]
87. Helmke BP, Goldman RD, Davies PF. Rapid displacement of vimentin intermediate filaments in living endothelial cells exposed to flow. *Circ Res.* 2000; 86(7):745–752. [PubMed: 10764407]
88. Feaver RE, Gelfand BD, Wang C, Schwartz MA, Blackman BR. Atheroprone hemodynamics regulate fibronectin deposition to create positive feedback that sustains endothelial inflammation. *Circ Res.* 2010; 106(11):1703–1711. [PubMed: 20378855]
89. Frangos JA, Eskin SG, McIntire LV, Ives CL. Flow effects on prostacyclin production by cultured human endothelial cells. *Science.* 1985; 227(4693):1477–1479. [PubMed: 3883488]
90. Barbee KA, Davies PF, Lal R. Shear stress-induced reorganization of the surface topography of living endothelial cells imaged by atomic force microscopy. *Circ Res.* 1994; 74(1):163–171. [PubMed: 8261591]
91. Davies PF, Remuzzi A, Gordon EJ, Dewey CF Jr, Gimbrone MA Jr. Turbulent fluid shear stress induces vascular endothelial cell turnover in vitro. *Proc Natl Acad Sci USA.* 1986; 83(7):2114–2117. [PubMed: 3457378]
92. Sun RJ, Muller S, Stoltz JF, Wang X. Shear stress induces caveolin-1 translocation in cultured endothelial cells. *Eur Biophys J.* 2002; 30(8):605–611. [PubMed: 11908851]
93. Yoshikawa N, Ariyoshi H, Ikeda M, Sakon M, Kawasaki T, Monden M. Shear-stress causes polarized change in cytoplasmic calcium concentration in human umbilical vein endothelial cells (HUVECs). *Cell Calcium.* 1997; 22(3):189–194. [PubMed: 9330789]
94. Butler PJ, Tsou TC, Li JY, Usami S, Chien S. Rate sensitivity of shear-induced changes in the lateral diffusion of endothelial cell membrane lipids: a role for membrane perturbation in shear-induced MAPK activation. *FASEB J.* 2002; 16(2):216–218. [PubMed: 11744620]
95. Wuensch T, Thilo F, Krueger K, Scholze A, Ristow M, Tepel M. High glucose-induced oxidative stress increases transient receptor potential channel expression in human monocytes. *Diabetes.* 2010; 59(4):844–849. [PubMed: 20068131]
96. Thilo F, Vorderwulbecke BJ, Marki A, et al. Pulsatile atheroprone shear stress affects the expression of transient receptor potential channels in human endothelial cells. *Hypertension.* 2012; 59(6):1232–1240. [PubMed: 22566504]
97. Bardell TK, Barker EL. Activation of TRPC6 channels promotes endocannabinoid biosynthesis in neuronal CAD cells. *Neurochem Int.* 2010; 57(1):76–83. [PubMed: 20466028]
98. Kronstein R, Seebach J, Grossklaus S, et al. Caveolin-1 opens endothelial cell junctions by targeting catenins. *Cardiovasc Res.* 2012; 93(1):130–140. [PubMed: 21960684]
99. Graziani A, Poteser M, Heupel WM, et al. Cell-cell contact formation governs Ca²⁺ signaling by TRPC4 in the vascular endothelium: evidence for a regulatory TRPC4-beta-catenin interaction. *J Biol Chem.* 2010; 285(6):4213–4223. [PubMed: 19996314]
100. Inoue R, Jensen LJ, Jian Z, et al. Synergistic activation of vascular TRPC6 channel by receptor and mechanical stimulation via phospholipase C/diacylglycerol and phospholipase A2/omega-hydroxylase/20-HETE pathways. *Circ Res.* 2009; 104(12):1399–1409. [PubMed: 19443836]
101. Spassova MA, Hewavitharana T, Xu W, Soboloff J, Gill DL. A common mechanism underlies stretch activation and receptor activation of TRPC6 channels. *Proc Natl Acad Sci USA.* 2006; 103(44):16586–16591. [PubMed: 17056714]
102. Gottlieb P, Folgering J, Maroto R, et al. Revisiting TRPC1 and TRPC6 mechanosensitivity. *Pflugers Arch.* 2008; 455(6):1097–1103. [PubMed: 17957383]
103. Mederos y Schnitzler M, Storch U, Meibers S, et al. Gq-coupled receptors as mechanosensors mediating myogenic vasoconstriction. *EMBO J.* 2008; 27(23):3092–3103. [PubMed: 18987636]
104. Melchior B, Frangos JA. Galphaq/11-mediated intracellular calcium responses to retrograde flow in endothelial cells. *Am J Physiol Cell Physiol.* 2012; 303(4):C467–C473. [PubMed: 22700794]
105. Storch U, Mederos Y, Schnitzler M, Gudermann T. G protein-mediated stretch reception. *Am J Physiol Heart Circ Physiol.* 2012; 302(6):H1241–H1249. [PubMed: 22227128]
106. Seong J, Lu S, Ouyang M, et al. Visualization of Src activity at different compartments of the plasma membrane by FRET imaging. *Chem Biol.* 2009; 16(1):48–57. [PubMed: 19171305]

107. Okuda M, Takahashi M, Suero J, et al. Shear stress stimulation of p130(cas) tyrosine phosphorylation requires calcium-dependent c-Src activation. *J Biol Chem.* 1999; 274(38): 26803–26809. [PubMed: 10480886]
108. Takahashi M, Berk BC. Mitogen-activated protein kinase (ERK1/2) activation by shear stress and adhesion in endothelial cells. Essential role for a herbimycin-sensitive kinase. *J Clin Invest.* 1996; 98(11):2623–2631. [PubMed: 8958227]
109. Rangaswami H, Schwappacher R, Marathe N, et al. Cyclic GMP and protein kinase G control a Src-containing mechanosome in osteoblasts. *Sci Signal.* 2010; 3(153):ra91. [PubMed: 21177494]
110. Gupta SK, Gallego C, Johnson GL, Heasley LE. MAP kinase is constitutively activated in gip2 and src transformed rat 1a fibroblasts. *J Biol Chem.* 1992; 267(12):7987–7990. [PubMed: 1314814]
111. Mansour SJ, Matten WT, Hermann AS, et al. Transformation of mammalian cells by constitutively active MAP kinase kinase. *Science.* 1994; 265(5174):966–970. [PubMed: 8052857]
112. Lenormand P, Sardet C, Pages G, L'Allemain G, Brunet A, Pouyssegur J. Growth factors induce nuclear translocation of MAP kinases (p42mapk and p44mapk) but not of their activator MAP kinase kinase (p45mapkk) in fibroblasts. *J Cell Biol.* 1993; 122(5):1079–1088. [PubMed: 8394845]
113. Ni CW, Wang DL, Lien SC, Cheng JJ, Chao YJ, Hsieh HJ. Activation of PKC-epsilon and ERK1/2 participates in shear-induced endothelial MCP-1 expression that is repressed by nitric oxide. *J Cell Physiol.* 2003; 195(3):428–434. [PubMed: 12704652]
114. Thomas SM, Brugge JS. Cellular functions regulated by Src family kinases. *Annu Rev Cell Dev Biol.* 1997; 13:513–609. [PubMed: 9442882]
115. Berdeaux RL, Diaz B, Kim L, Martin GS. Active Rho is localized to podosomes induced by oncogenic Src and is required for their assembly and function. *J Cell Biol.* 2004; 166(3):317–323. [PubMed: 15289494]
116. Huvneers S, Oldenburg J, Spanjaard E, et al. Vinculin associates with endothelial VE-cadherin junctions to control force-dependent remodeling. *J Cell Biol.* 2012; 196(5):641–652. [PubMed: 22391038]
117. Klemke RL, Cai S, Giannini AL, Gallagher PJ, de Lanerolle P, Cheresch DA. Regulation of cell motility by mitogen-activated protein kinase. *J Cell Biol.* 1997; 137(2):481–492. [PubMed: 9128257]
118. Zacharias DA, Violin JD, Newton AC, Tsien RY. Partitioning of lipid-modified monomeric GFPs into membrane microdomains of live cells. *Science.* 2002; 296(5569):913–916. [PubMed: 11988576]
119. Ohno M, Gibbons GH, Dzau VJ, Cooke JP. Shear stress elevates endothelial cGMP. Role of a potassium channel and G protein coupling. *Circulation.* 1993; 88(1):193–197. [PubMed: 8391400]
120. Jo H, Sipos K, Go YM, Law R, Rong J, McDonald JM. Differential effect of shear stress on extracellular signal-regulated kinase and N-terminal Jun kinase in endothelial cells. Gi2- and Gbeta/gamma-dependent signaling pathways. *J Biol Chem.* 1997; 272(2):1395–1401. [PubMed: 8995450]
121. Bard F, Patel U, Levy JB, Jurdic P, Horne WC, Baron R. Molecular complexes that contain both c-Cbl and c-Src associate with Golgi membranes. *Eur J Cell Biol.* 2002; 81(1):26–35. [PubMed: 11893076]
122. Horne WC, Neff L, Chatterjee D, Lomri A, Levy JB, Baron R. Osteoclasts express high levels of pp60c-src in association with intracellular membranes. *J Cell Biol.* 1992; 119(4):1003–1013. [PubMed: 1385441]
123. Krueger JG, Wang E, Garber EA, Goldberg AR. Differences in intracellular location of pp60src in rat and chicken cells transformed by Rous sarcoma virus. *Proc Natl Acad Sci USA.* 1980; 77(7): 4142–4146. [PubMed: 6254012]
124. Redmond T, Brott BK, Jove R, Welsh MJ. Localization of the viral and cellular Src kinases to perinuclear vesicles in fibroblasts. *Cell Growth Differ.* 1992; 3(9):567–576. [PubMed: 1384654]

125. Kaplan KB, Swedlow JR, Varmus HE, Morgan DO. Association of p60c-src with endosomal membranes in mammalian fibroblasts. *J Cell Biol.* 1992; 118(2):321–333. [PubMed: 1378446]
126. Kawakatsu H, Sakai T, Takagaki Y, et al. A new monoclonal antibody which selectively recognizes the active form of Src tyrosine kinase. *J Biol Chem.* 1996; 271(10):5680–5685. [PubMed: 8621432]
127. Mukherjee A, Arnaud L, Cooper JA. Lipid-dependent recruitment of neuronal Src to lipid rafts in the brain. *J Biol Chem.* 2003; 278(42):40806–40814. [PubMed: 12912979]
128. Hitosugi T, Sato M, Sasaki K, Umezawa Y. Lipid raft specific knockdown of SRC family kinase activity inhibits cell adhesion and cell cycle progression of breast cancer cells. *Cancer Res.* 2007; 67(17):8139–8148. [PubMed: 17804726]
129. Kasai A, Shima T, Okada M. Role of Src family tyrosine kinases in the down-regulation of epidermal growth factor signaling in PC12 cells. *Genes Cells.* 2005; 10(12):1175–1187. [PubMed: 16324154]
130. Fincham VJ, Unlu M, Brunton VG, Pitts JD, Wyke JA, Frame MC. Translocation of Src kinase to the cell periphery is mediated by the actin cytoskeleton under the control of the Rho family of small G proteins. *J Cell Biol.* 1996; 135(6 Pt 1):1551–1564. [PubMed: 8978822]
131. Timpson P, Jones GE, Frame MC, Brunton VG. Coordination of cell polarization and migration by the Rho family GTPases requires Src tyrosine kinase activity. *Curr Biol.* 2001; 11(23):1836–1846. [PubMed: 11728306]
132. Sandilands E, Cans C, Fincham VJ, et al. RhoB and actin polymerization coordinate Src activation with endosome-mediated delivery to the membrane. *Dev Cell.* 2004; 7(6):855–869. [PubMed: 15572128]
133. Fincham VJ, Brunton VG, Frame MC. The SH3 domain directs acto-myosin-dependent targeting of v-Src to focal adhesions via phosphatidylinositol 3-kinase. *Mol Cell Biol.* 2000; 20(17):6518–6536. [PubMed: 10938128]
134. Fincham VJ, Frame MC. The catalytic activity of Src is dispensable for translocation to focal adhesions but controls the turnover of these structures during cell motility. *EMBO J.* 1998; 17(1):81–92. [PubMed: 9427743]
135. Lasserre R, Guo XJ, Conchonaud F, et al. Raft nanodomains contribute to Akt/PKB plasma membrane recruitment and activation. *Nat Chem Biol.* 2008; 4(9):538–547. [PubMed: 18641634]
136. Sandilands E, Brunton VG, Frame MC. The membrane targeting and spatial activation of Src, Yes and Fyn is influenced by palmitoylation and distinct RhoB/RhoD endosome requirements. *J Cell Sci.* 2007; 120(Pt 15):2555–2564. [PubMed: 17623777]
137. Simons K, Toomre D. Lipid rafts and signal transduction. *Nat Rev Mol Cell Biol.* 2000; 1(1):31–39. [PubMed: 11413487]
138. Arcaro A, Aubert M, Espinosa del Hierro ME, et al. Critical role for lipid raft-associated Src kinases in activation of PI3K-Akt signalling. *Cell Signal.* 2007; 19(5):1081–1092. [PubMed: 17275257]
139. Na S, Collin O, Chowdhury F, et al. Rapid signal transduction in living cells is a unique feature of mechanotransduction. *Proc Natl Acad Sci USA.* 2008; 105(18):6626–6631. [PubMed: 18456839]
140. Shima T, Nada S, Okada M. Transmembrane phosphoprotein Cbp senses cell adhesion signaling mediated by Src family kinase in lipid rafts. *Proc Natl Acad Sci USA.* 2003; 100(25):14897–14902. [PubMed: 14645715]
141. Lichtenberg D, Goni FM, Heerklotz H. Detergent-resistant membranes should not be identified with membrane rafts. *Trends Biochem Sci.* 2005; 30(8):430–436. [PubMed: 15996869]
142. Bradshaw JM, Mitaxov V, Waksman G. Investigation of phosphotyrosine recognition by the SH2 domain of the Src kinase. *J Mol Biol.* 1999; 293(4):971–985. [PubMed: 10543978]
143. Rodriguez OC, Schaefer AW, Mandato CA, Forscher P, Bement WM, Waterman-Storer CM. Conserved microtubule-actin interactions in cell movement and morphogenesis. *Nat Cell Biol.* 2003; 5(7):599–609. [PubMed: 12833063]
144. Ardern H, Sandilands E, Machesky LM, Timpson P, Frame MC, Brunton VG. Src-dependent phosphorylation of Scar1 promotes its association with the Arp2/3 complex. *Cell Motil Cytoskeleton.* 2006; 63(1):6–13. [PubMed: 16317717]

145. Sheetz MP. Cell control by membrane-cytoskeleton adhesion. *Nat Rev Mol Cell Biol.* 2001; 2(5): 392–396. [PubMed: 11331914]
146. Seong J, Ouyang M, Kim T, et al. Detection of focal adhesion kinase activation at membrane microdomains by fluorescence resonance energy transfer. *Nat Commun.* 2011; 2:406. [PubMed: 21792185]
147. Okegawa T, Li Y, Pong RC, Hsieh JT. Cell adhesion proteins as tumor suppressors. *J Urol.* 2002; 167(4):1836–1843. [PubMed: 11912444]
148. Dejana E, Bazzoni G, Lampugnani MG. Vascular endothelial (VE)-cadherin: only an intercellular glue? *Exp Cell Res.* 1999; 252(1):13–19. [PubMed: 10502395]
149. Gumbiner BM. Cell adhesion: the molecular basis of tissue architecture and morphogenesis. *Cell.* 1996; 84(3):345–357. [PubMed: 8608588]
150. Geiger B, Ayalon O. Cadherins. *Annu Rev Cell Biol.* 1992; 8:307–332. [PubMed: 1476802]
151. Yamada KM, Geiger B. Molecular interactions in cell adhesion complexes. *Curr Opin Cell Biol.* 1997; 9(1):76–85. [PubMed: 9013677]
152. Hamaguchi M, Matsuyoshi N, Ohnishi Y, Gotoh B, Takeichi M, Nagai Y. p60v-src causes tyrosine phosphorylation and inactivation of the N-cadherin-catenin cell adhesion system. *EMBO J.* 1993; 12(1):307–314. [PubMed: 8381351]
153. Matsuyoshi N, Hamaguchi M, Taniguchi S, Nagafuchi A, Tsukita S, Takeichi M. Cadherin-mediated cell-cell adhesion is perturbed by v-src tyrosine phosphorylation in metastatic fibroblasts. *J Cell Biol.* 1992; 118(3):703–714. [PubMed: 1639852]
154. Behrens J, Vakaet L, Friis R, et al. Loss of epithelial differentiation and gain of invasiveness correlates with tyrosine phosphorylation of the E-cadherin/beta-catenin complex in cells transformed with a temperature-sensitive v-SRC gene. *J Cell Biol.* 1993; 120(3):757–766. [PubMed: 8425900]
155. Avizienyte E, Fincham VJ, Brunton VG, Frame MC. Src SH3/2 domain-mediated peripheral accumulation of Src and phospho-myosin is linked to deregulation of E-cadherin and the epithelial-mesenchymal transition. *Mol Biol Cell.* 2004; 15(6):2794–2803. [PubMed: 15075377]
156. Li YS, Shyy JY, Li S, et al. The Ras-JNK pathway is involved in shear-induced gene expression. *Mol Cell Biol.* 1996; 16(11):5947–5954. [PubMed: 8887624]
157. Luo BH, Carman CV, Springer TA. Structural basis of integrin regulation and signaling. *Annu Rev Immunol.* 2007; 25:619–647. [PubMed: 17201681]
158. Mitra SK, Hanson DA, Schlaepfer DD. Focal adhesion kinase: in command and control of cell motility. *Nat Rev Mol Cell Biol.* 2005; 6(1):56–68. [PubMed: 15688067]
159. Mitra SK, Schlaepfer DD. Integrin-regulated FAK-Src signaling in normal and cancer cells. *Curr Opin Cell Biol.* 2006; 18(5):516–523. [PubMed: 16919435]
160. Seong J, Tajik A, Sun J, et al. Distinct biophysical mechanisms of focal adhesion kinase mechanoactivation by different extracellular matrix proteins. *Proc Natl Acad Sci USA.* 2013; 110(48):19372–19377. [PubMed: 24222685]
161. Critchley DR. Cytoskeletal proteins talin and vinculin in integrin-mediated adhesion. *Biochem Soc Trans.* 2004; 32(Pt 5):831–836. [PubMed: 15494027]
162. Critchley DR. Genetic, biochemical and structural approaches to talin function. *Bio-chem Soc Trans.* 2005; 33(Pt 6):1308–1312.
163. Bershadsky AD, Balaban NQ, Geiger B. Adhesion-dependent cell mechanosensitivity. *Annu Rev Cell Dev Biol.* 2003; 19:677–695. [PubMed: 14570586]
164. Geiger B, Spatz JP, Bershadsky AD. Environmental sensing through focal adhesions. *Nat Rev Mol Cell Biol.* 2009; 10(1):21–33. [PubMed: 19197329]
165. Nguyen AW, Daugherty PS. Evolutionary optimization of fluorescent proteins for intracellular FRET. *Nat Biotechnol.* 2005; 23(3):355–360. [PubMed: 15696158]
166. Ouyang M, Sun J, Chien S, Wang Y. Determination of hierarchical relationship of Src and Rac at subcellular locations with FRET biosensors. *Proc Natl Acad Sci USA.* 2008; 105(38):14353–14358. [PubMed: 18799748]

167. Kawai H, Suzuki T, Kobayashi T, et al. Simultaneous real-time detection of initiator-and effector-caspase activation by double fluorescence resonance energy transfer analysis. *J Pharmacol Sci*. 2005; 97(3):361–368. [PubMed: 15750288]
168. Peyker A, Rocks O, Bastiaens PI. Imaging activation of two Ras isoforms simultaneously in a single cell. *Chembiochem*. 2005; 6(1):78–85. [PubMed: 15637661]
169. Wu X, Simone J, Hewgill D, Siegel R, Lipsky PE, He L. Measurement of two caspase activities simultaneously in living cells by a novel dual FRET fluorescent indicator probe. *Cytometry A*. 2006; 69(6):477–486. [PubMed: 16683263]
170. Ai HW, Hazelwood KL, Davidson MW, Campbell RE. Fluorescent protein FRET pairs for ratiometric imaging of dual biosensors. *Nat Methods*. 2008; 5(5):401–403. [PubMed: 18425137]
171. Shaner NC, Campbell RE, Steinbach PA, Giepmans BN, Palmer AE, Tsien RY. Improved monomeric red, orange and yellow fluorescent proteins derived from *Discosoma* sp. red fluorescent protein. *Nat Biotechnol*. 2004; 22(12):1567–1572. [PubMed: 15558047]
172. Shaner NC, Lin MZ, McKeown MR, et al. Improving the photostability of bright monomeric orange and red fluorescent proteins. *Nat Methods*. 2008; 5(6):545–551. [PubMed: 18454154]
173. Shaner NC, Steinbach PA, Tsien RY. A guide to choosing fluorescent proteins. *Nat Methods*. 2005; 2(12):905–909. [PubMed: 16299475]
174. Goedhart J, Vermeer JE, Adjobo-Hermans MJ, van Weeren L, Gadella TW Jr. Sensitive detection of p65 homodimers using red-shifted and fluorescent protein-based FRET couples. *PLoS One*. 2007; 2(10):e1011. [PubMed: 17925859]
175. Grant DM, Zhang W, McGhee EJ, et al. Multiplexed FRET to image multiple signaling events in live cells. *Biophys J*. 2008; 95(10):L69–L71. [PubMed: 18757561]
176. Niino Y, Hotta K, Oka K. Simultaneous live cell imaging using dual FRET sensors with a single excitation light. *PLoS One*. 2009; 4(6):e6036. [PubMed: 19551140]
177. Ouyang M, Huang H, Shaner NC, et al. Simultaneous visualization of protumorigenic Src and MT1-MMP activities with fluorescence resonance energy transfer. *Cancer Res*. 2010; 70(6):2204–2212. [PubMed: 20197470]
178. Wallrabe H, Periasamy A. Imaging protein molecules using FRET and FLIM microscopy. *Curr Opin Biotechnol*. 2005; 16(1):19–27. [PubMed: 15722011]
179. Chao LK, Clegg RM. Foerster resonance energy transfer (FRET) for proteins Wiley Encyclopedia of Chemical Biology Advanced Review. 2008:0.
180. Clegg, RM. Fluorescence resonance energy transfer. In: Wang, XF., Herman, B., editors. *Fluorescence Imaging Spectroscopy and Microscopy*. New York: John Wiley & Sons, Inc; 1996. p. 179-252.
181. Clegg, RM. Nuts and bolts of excitation energy migration and energy transfer. In: Papageorgiou, GC., Govindjee, editors. *Chlorophyll a Fluorescence: A Signature of Photosynthesis*. The Netherlands: Springer; 2005. p. 83-105.
182. Kraynov VS, Chamberlain C, Bokoch GM, Schwartz MA, Slabaugh S, Hahn KM. Localized Rac activation dynamics visualized in living cells. *Science*. 2000; 290(5490):333–337. [PubMed: 11030651]
183. Tzima E, Del Pozo MA, Kiosses WB, et al. Activation of Rac1 by shear stress in endothelial cells mediates both cytoskeletal reorganization and effects on gene expression. *EMBO J*. 2002; 21(24):6791–6800. [PubMed: 12486000]
184. Tzima E, Kiosses WB, del Pozo MA, Schwartz MA. Localized cdc42 activation, detected using a novel assay, mediates microtubule organizing center positioning in endothelial cells in response to fluid shear stress. *J Biol Chem*. 2003; 278(33):31020–31023. [PubMed: 12754216]
185. Ganguli A, Persson L, Palmer IR, et al. Distinct NF-kappaB regulation by shear stress through Ras-dependent IkappaBalpha oscillations: real-time analysis of flow-mediated activation in live cells. *Circ Res*. 2005; 96(6):626–634. [PubMed: 15731464]
186. Eyckmans J, Boudou T, Yu X, Chen CS. A hitchhiker's guide to mechanobiology. *Dev Cell*. 2011; 21(1):35–47. [PubMed: 21763607]
187. Axelrod D, Koppel DE, Schlessinger J, Elson E, Webb WW. Mobility measurement by analysis of fluorescence photobleaching recovery kinetics. *Biophys J*. 1976; 16(9):1055–1069. [PubMed: 786399]

188. Klonis N, Rug M, Harper I, Wickham M, Cowman A, Tilley L. Fluorescence photobleaching analysis for the study of cellular dynamics. *Eur Biophys J.* 2002; 31(1):36–51. [PubMed: 12046896]
189. Lippincott-Schwartz J, Snapp E, Kenworthy A. Studying protein dynamics in living cells. *Nat Rev Mol Cell Biol.* 2001; 2(6):444–456. [PubMed: 11389468]
190. Lippincott-Schwartz J, Patterson GH. Development and use of fluorescent protein markers in living cells. *Science.* 2003; 300(5616):87–91. [PubMed: 12677058]
191. Phair RD, Misteli T. Kinetic modelling approaches to in vivo imaging. *Nat Rev Mol Cell Biol.* 2001; 2(12):898–907. [PubMed: 11733769]
192. Nehls S, Snapp EL, Cole NB, et al. Dynamics and retention of misfolded proteins in native ER membranes. *Nat Cell Biol.* 2000; 2(5):288–295. [PubMed: 10806480]
193. Carrero G, McDonald D, Crawford E, de Vries G, Hendzel MJ. Using FRAP and mathematical modeling to determine the in vivo kinetics of nuclear proteins. *Methods.* 2003; 29(1):14–28. [PubMed: 12543068]
194. Sbalzarini IF, Mezzacasa A, Helenius A, Koumoutsakos P. Effects of organelle shape on fluorescence recovery after photobleaching. *Biophys J.* 2005; 89(3):1482–1492. [PubMed: 15951382]
195. Sbalzarini IF, Hayer A, Helenius A, Koumoutsakos P. Simulations of (an)isotropic diffusion on curved biological surfaces. *Biophys J.* 2006; 90(3):878–885. [PubMed: 16284262]
196. Ulrich M, Kappel C, Beaudouin J, Hezel S, Ulrich J, Eils R. Tropical-parameter estimation and simulation of reaction-diffusion models based on spatio-temporal microscopy images. *Bioinformatics.* 2006; 22(21):2709–2710. [PubMed: 16940327]
197. Beaudouin J, Mora-Bermudez F, Klee T, Daigle N, Ellenberg J. Dissecting the contribution of diffusion and interactions to the mobility of nuclear proteins. *Biophys J.* 2006; 90(6):1878–1894. [PubMed: 16387760]
198. Houtsmuller AB, Rademakers S, Nigg AL, Hoogstraten D, Hoeijmakers JH, Vermeulen W. Action of DNA repair endonuclease ERCC1/XPF in living cells. *Science.* 1999; 284(5416):958–961. [PubMed: 10320375]
199. Farla P, Hersmus R, Geverts B, et al. The androgen receptor ligand-binding domain stabilizes DNA binding in living cells. *J Struct Biol.* 2004; 147(1):50–61. [PubMed: 15109605]
200. Sniekers YH, van Donkelaar CC. Determining diffusion coefficients in inhomogeneous tissues using fluorescence recovery after photobleaching. *Biophys J.* 2005; 89(2):1302–1307. [PubMed: 15894637]
201. Barondeau DP, Kassmann CJ, Tainer JA, Getzoff ED. Structural chemistry of a green fluorescent protein Zn biosensor. *J Am Chem Soc.* 2002; 124(14):3522–3524. [PubMed: 11929238]
202. Costa KD, Hunter PJ, Rogers JM, Guccione JM, Waldman LK, McCulloch AD. A three-dimensional finite element method for large elastic deformations of ventricular myocardium: I—cylindrical and spherical polar coordinates. *J Biomech Eng.* 1996; 118(4):452–463. [PubMed: 8950648]
203. Sadegh Zadeh K, Elman HC, Montas HJ, Shirmohammadi A. A finite element model for protein transport in vivo. *Biomed Eng Online.* 2007; 6:24. [PubMed: 17598901]
204. Zitova B, Flusser J. Image registration methods: a survey. *Image Vis Comput.* 2003; 21(11):977–1000.
205. Jagalur M, Pal C, Learned-Miller E, Zoeller RT, Kulp D. Analyzing in situ gene expression in the mouse brain with image registration, feature extraction and block clustering. *BMC Bioinformatics.* 2007; 8(Suppl 10):S5.
206. Yeo MG, Partridge MA, Ezratty EJ, Shen Q, Gundersen GG, Marcantonio EE. Src SH2 arginine 175 is required for cell motility: specific focal adhesion kinase targeting and focal adhesion assembly function. *Mol Cell Biol.* 2006; 26(12):4399–4409. [PubMed: 16738308]
207. Dormann D, Libotte T, Weijer CJ, Bretschneider T. Simultaneous quantification of cell motility and protein-membrane-association using active contours. *Cell Motil Cytoskeleton.* 2002; 52(4):221–230. [PubMed: 12112136]

208. Dubin-Thaler BJ, Giannone G, Dobereiner HG, Sheetz MP. Nanometer analysis of cell spreading on matrix-coated surfaces reveals two distinct cell states and STEPs. *Biophys J.* 2004; 86(3): 1794–1806. [PubMed: 14990505]
209. Cavalcanti-Adam EA, Volberg T, Micoulet A, Kessler H, Geiger B, Spatz JP. Cell spreading and focal adhesion dynamics are regulated by spacing of integrin ligands. *Biophys J.* 2007; 92(8): 2964–2974. [PubMed: 17277192]
210. Shaoying, Lu, Tae-jin, Kim, Chih-En, Chen, et al. Computational analysis of the spatio-temporal coordination of polarized PI3K and Rac1 activities in micropatterned live cells. *PLoS One.* 2011; 6(6):e21293. [PubMed: 21738630]

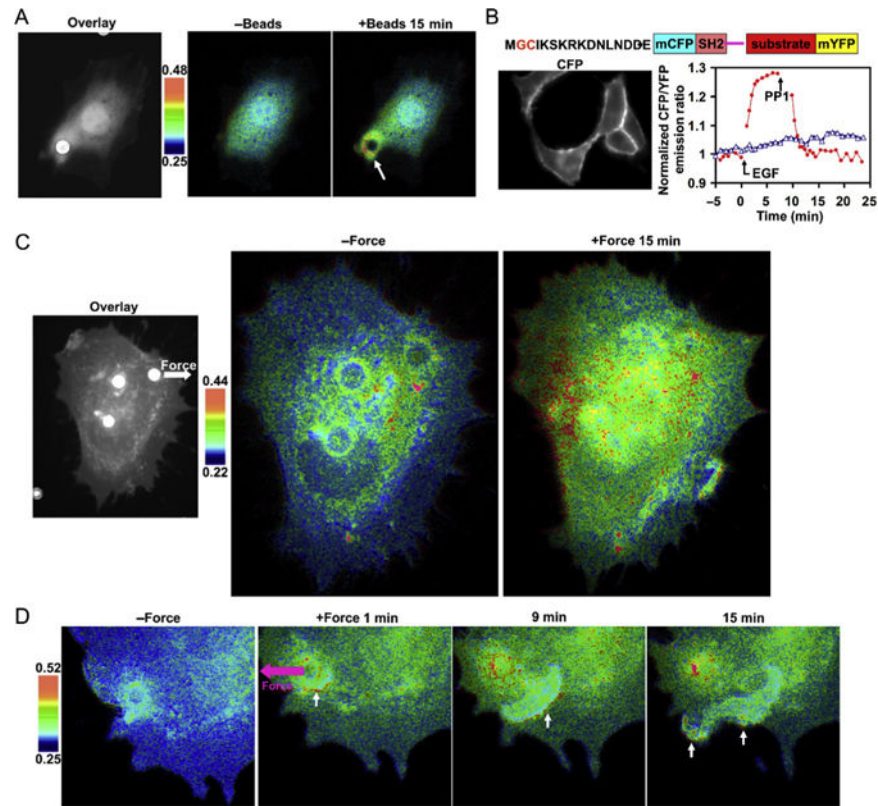
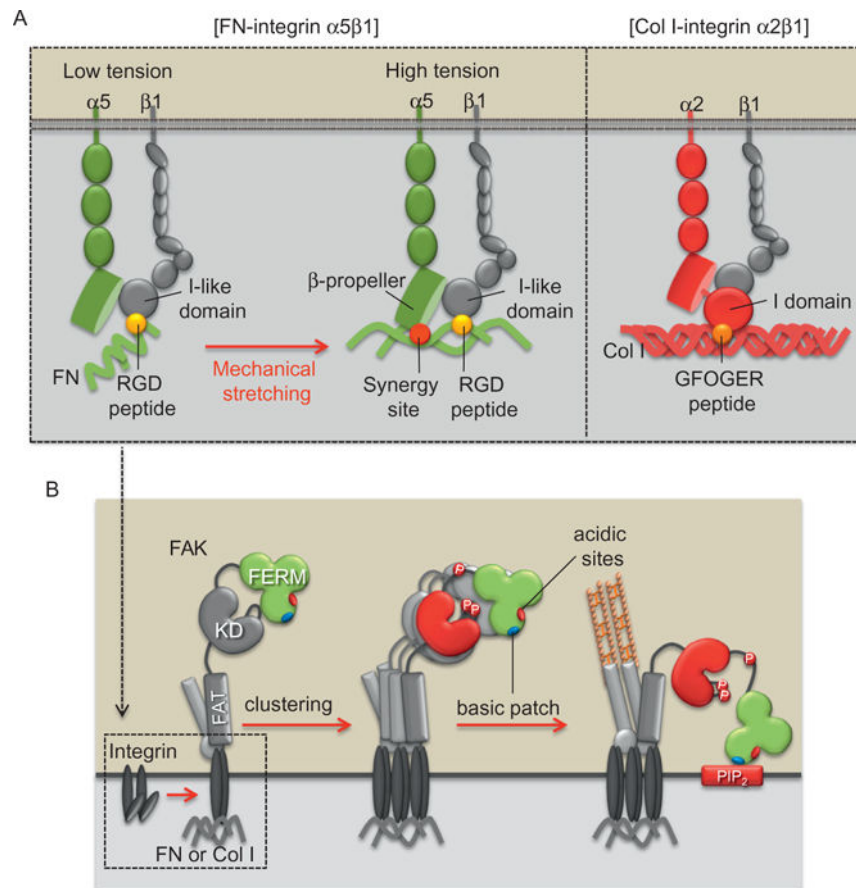


Figure 2.1.

Directional and long-range propagation of Src induced by mechanical force. (A) A fibronectin-coated bead (white spot from phase contrast image overlaid on CFP cell image) induced FRET responses around the bead. White arrow points to the spot with activated Src. Color bar represents CFP/YFP emission ratio values. (B) The schematic diagram in the upper panel shows the design strategy of membrane targeting. The CFP-only image on the left shows the effective tethering of the reporter on the plasma membrane. The EGF-induced FRET responses of the reporter is reversed by PP1 (red line) and prevented by pretreatment with PP1 (blue line). (C) Laser-tweezer traction on the bead at the upper right corner of the cell (shown on the left) caused FRET responses. White arrow represents force direction. (D) FRET responses of a cell with clear directional wave propagation away from the site of mechanical stimulation. This research was originally published in the Nature Journal.³⁴

**Figure 2.2.**

Proposed model of FAK mechanoactivation mechanisms via different ECM and integrin subtypes during cell adhesion process. (A) Integrin $\alpha 5 \beta 1$ can be fully activated in the tensioned state where both RGD peptide (yellow circle [white in print version]) and synergy site (red circle [dark gray in print version]) bind to $\alpha 5$ and $\beta 1$ subunits, respectively. Because FN synergy site is exposed only in the high-tensional state, the FAK activation via integrin $\alpha 5 \beta 1$ is dependent on the mechanical environment. In contrast, integrin $\alpha 2 \beta 1$ can directly bind to the constitutively exposed GFOGER motif (orange circle [light gray in print version]) in Col I, thus causing the activation of integrin $\alpha 2 \beta 1$ and FAK independent of mechanical tension. (B) Integrin activation can recruit and induce the transphosphorylation of FAK. This leads to the FAK activation, which is maintained by the interaction between the FERM basic patch (blue oval [light gray in print version]) and PIP₂ to prevent the inhibitory interaction of myosin II with FERM acidic sites (red oval [dark gray in print version]). This research was originally published in Nature Communication.¹⁴⁶

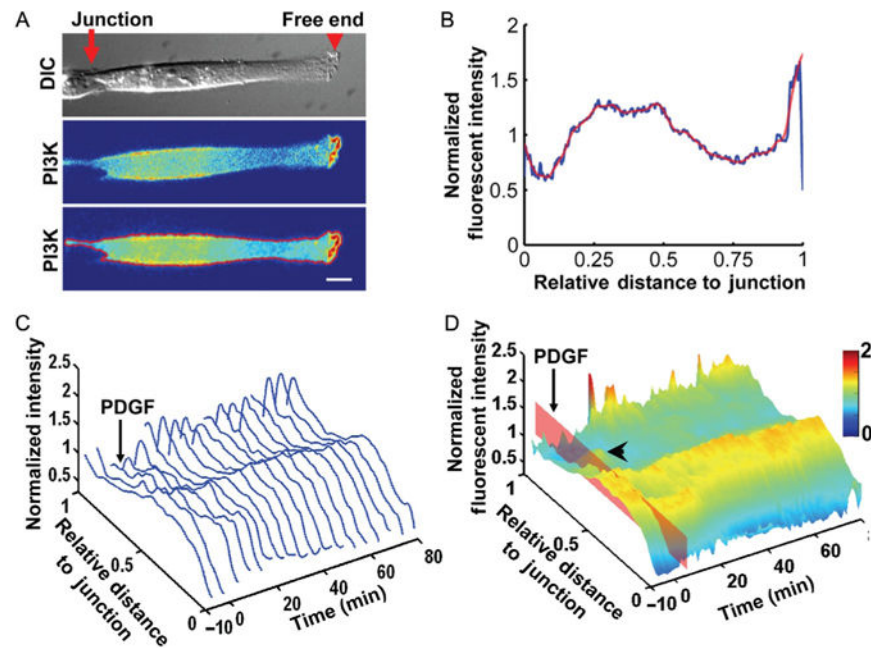


Figure 2.3.

The quantification methods and protein localization results. (A) The alignment and outline of a cell before quantification. Top panel: The DIC image of a cell with a junction connecting to a neighboring cell on a patterned FN strip and a free end capable of lamellipodial protrusion. Middle panel: The fluorescence image shows the intensity distribution of PH-Akt-GFP expressed in the cell of interest. Bottom panel: The cell was rotated and aligned along a horizontal direction, and the boundary of the cell calculated and overlaid in red with the fluorescence intensity image. Scale bar: 10 μm . (B) The normalized fluorescence intensity of PH-Akt-GFP plotted against the relative distance to the junction end with the blue and red lines representing the raw and smoothed data, respectively. (C) The sequence of the normalized fluorescence intensity curves arranged along the time axis with a 3D view. The platelet-derived growth factor (PDGF) stimulation was applied at 0 min. (D) The 3D intensity surface of PI3K activity landscape was color-coded by the fluorescence intensity values and visualized as a function of time and distance to the junction end, based on the data in (C). The time of PDGF stimulation is indicated by the red plane. A transient secondary peak can be observed between the cell body and the free end (arrowhead). This research was originally published in PLoS One.²¹⁰